Slow Slip Events in Mexico: A Historical Perspective

Víctor M. Cruz-Atienza[a]*, Sara Franco[a], Vladimir Kostoglodov[a], Josué Tago[b], Ekaterina Kazachkina[a], Jorge Real[a], Carlos Villafuerte[a] and Raymundo Plata-Martínez[a]

[a]Instituto de Geofísica, Universidad Nacional Autónoma de México, Mexico
[b]Facultad de Ingeniería, Universidad Nacional Autónoma de México, Mexico

*Corresponding author: cruz@igeofisica.unam.mx

This manuscript has not been peer-reviewed and was submitted to Tectonophysics in July 2025

Abstract

This paper introduces a historical catalogue of slow slip events (SSE) for the Mexican subduction zone. The catalogue incorporates all 25 SSEs recorded since they were discovered in 1997. The inversion of GPS data for ten SSEs in Guerrero and five in Oaxaca reveals a clear slow slip segmentation along the Middle America Trench, with slip maxima between 30 and 40 km depth in both regions. SSEs in Guerrero are significantly larger, with $M_w = 7.14 \pm 0.18$ and a duration of 10.3 ± 6.5 months, whereas in Oaxaca, $M_w = 6.84 \pm 0.16$ with a duration of 7.0 ± 4.3 months. Such discrepancy results from the subhorizontal geometry of the Cocos Plate in Guerrero, which favors a more extensive SSE habitat. The extent and along-strike segmentation of SSEs appear to be structurally controlled by the subduction of the Orozco and O'Gorman fracture zones. For the inversions, we used consistent GPS data processing that preserves the North American reference frame and the actual SSEs crustal rebounds. All data were curated to minimize seasonal noise, and interpreted throughout the ELADIN inversion method. Five of the six most recent M7+ earthquakes in the region were preceded and most likely triggered by an SSE. This earthquake cluster began after a 17-year period of quiescence, during which large SSEs occurred. While the SSEs appear to be necessary for initiating large ruptures, this is not enough until sufficient energy has accumulated in the seismogenic zone. The Mexican seismic record since 1800 suggests that every ~15 years the subduction zone reaches a critical state in which SSEs become large earthquake triggers.

1. Introduction

Silent earthquakes in the Mexican subduction zone were discovered in the same year as Cascadia (Lawry et al., 2001; Dragert et al., 2001). Careful treatment and gradual interpretation of the GPS and InSAR data over the past 28 years have identified the regions of the plate interface where transient slow slip occurs between the subducting Cocos and the overriding North American plates (Brudzinski et al., 2007; Cavalié et al., 2013; Correa-Mora et al., 2009; Franco et al., 2005; Iglesias et al., 2004; Kostoglodov et al., 2010, 2003; Radiguet et al., 2012, 2011; Vergnolle et al., 2010; Walpersdorf et al., 2011). The difference in their behavior in the neighboring states of Guerrero and Oaxaca is clear. While the recurrence interval of slow slip events (SSE) in Guerrero was relatively regular at ~3.5 years until 2014 (Cotte et al., 2011), SSEs in Oaxaca occur more frequently (i.e., every 1-2 years) and are generally smaller in magnitude (Correa-Mora et al., 2009, 2008; Cruz-Atienza et al., 2021; Graham et al., 2016; Villafuerte et al., 2025). It appears that plate geometry and its petrologic implications play a relevant role in

this phenomenon. While in Guerrero the plate interface becomes subhorizontal at a depth of ~30 km, in Oaxaca, the Cocos Plate gradually transitions to a steep subduction geometry (Fasola et al., 2016; Pardo and Suarez, 1995; Pérez-Campos et al., 2008). This means that the depths conducive to slow slip instabilities (i.e., between ~20 and ~45 km) have a different range in the two states, with a significantly larger extension in Guerrero. An impermeable continental lower crust and overpressured fluids confinement around the interface may contribute to this clear differentiation of the SSE habitats (Audet and Kim, 2016; Cruz-Atienza et al., 2018b; Husker et al., 2018; Legrand et al., 2021; Manea and Manea, 2011). Apart from those in Guerrero and Oaxaca, no other convincing detections of SSEs have been made in the Mexican subduction zone using geodetic methods. Nucleation of large subduction earthquakes triggered by neighboring SSEs has been demonstrated in both states where the last six M7+ ruptures were preceded and likely triggered in most cases by a nearby aseismic event (Cruz-Atienza et al., 2025, 2021; Graham et al., 2014; Radiguet et al., 2016; Villafuerte et al., 2025), indicating that the seismic hazard may rise when slow slip transients occur.

Research dedicated to SSEs in Mexico has been carried out using various modelling frameworks and geodetic data processing over the years (e.g., Graham et al., 2014; Larson et al., 2007; Radiguet et al., 2016, 2012). The models used vary in terms of the geometry of the plate interface, the crustal model and the inversion techniques themselves, which have very dissimilar regularization methods. On the other hand, GPS data has evolved over time as well, initially being collected from occupation measurements to become continuous acquisition (Figure 1) in networks whose coverage has expanded over time. This makes it difficult to create a consistent and reliable SSE picture of the region, and to make direct and reliable comparisons between the events under study. While the evolution of observational coverage is an inherent aspect of history, consistent data processing and interpretation are a distinct possibility.

In this paper, we reexamine the history of the SSEs in the Mexican subduction zone, offering new interpretations in order to compile a comprehensive catalogue of the region. To this end, we analyze the historical GPS records of all events in Guerrero and Oaxaca (where data is available; e.g. Figure 1), applying consistent geodetic data processing and inversion techniques. This analysis provides an overview of the spatial extent and timing of SSEs, as well as their relationship with past earthquakes in the region.

Figure 1

2. Methods

2.1. GPS Data Treatment

Transient variations in the deformation pattern of subduction zones observed in GPS time series are interpreted as variations in the slip rate at the plate interface. Depending on the magnitude of these changes, the crust may undergo elastic rebound (i.e., stress drop) or simply decrease its stressing rate. In other words, depending on whether or not the slip rate overcomes the plate convergence, the medium will experience relaxation. In this context, the definition of an SSE is not straightforward. Does an SSE initiate at the moment the stress starts to fall or rather at the moment the loading rate starts to fall? Can we say that coupling drops

respond to the occurrence of (incipient) SSEs? From a fracture dynamics point of view, these two scenarios have very different implications.

Removing the inter-SSE GPS displacement linear trends from the data to quantify and interpret SSEs (i.e. to invert them) is a common practice (e.g., Cavalié et al., 2013; Radiguet et al., 2011, 2012). This procedure has three important implications for the outcome results: (1) the onset of the GPS displacement transients as the plate coupling begins to decrease (i.e., before the stress drop initiates) is interpreted as part of the total SSE slip distribution, (2) the resulting GPS time series lack a common reference frame implicit in the linear trends, and (3) the final SSE-associated GPS offsets are significantly larger than their values before the time series are detrended. As discussed by Cruz-Atienza et al. (2021) and Villafuerte et al. (2025), the inversion of this type of data results in a very significant overestimation of the SSE seismic moment (e.g., Ochi and Kato, 2013), which may have important implications for the strain budget over several SSE cycles.

A reliable assessment of the role of SSEs in the seismic cycle may come from inversions that preserve a common reference frame of the GPS data (i.e., where the inter-SSE linear trends are preserved), and thus where the SSE-associated offsets correspond to the actual relaxing slip at the interface where stress drop takes place (Cruz-Atienza et al., 2025, 2021; Ochi and Kato, 2013; Tago et al., 2021; Villafuerte et al., 2025). To be consistent, such an inversion procedure should simultaneously image the stressing (i.e., under coupling regime) and relaxing slip across the plate boundary.

The data is sourced from the GPS networks operated by the Mexican Seismological Service (SSN), the Department of Seismology of the Institute of Geophysics of UNAM and Tlalocnet (Cabral-Cano et al., 2018). The GPS position time series are estimated using the GIPSY 6.4 software package developed by Jet Propulsion Laboratory (Ries et al., 2015), following a Precise Point Positioning strategy (Zumberge et al., 1997). The station positions are defined in the International Terrestrial Reference Frame (ITRF, 2014). For daily processing, we used the Jet Propulsion Laboratory's final and non-fiducial products (orbits and clocks). The observables were generated using two model categories: (1) Earth models and (2) observation models. Earth models include tidal effects (i.e. solid tides, ocean loading and tides created by polar motion), Earth rotation (UT1), polar motion, nutation and precession. In contrast, observation models are associated with phase center offsets, tropospheric effects and timing errors (i.e. relativistic effects). The troposphere delay is estimated as a random walk process. This effect is divided into wet and dry components. The azimuthal gradient and the dry component are estimated using the GPT2 model (Lagler et al., 2013). The phase center variations of the antennas are considered via the antenna calibration files. For receiver antennas, the correction is estimated through the International GNSS Service (IGS) Antex file. We also applied a wide-lane phase bias to account for the ambiguity resolution.

In order to remove any outliers and then estimate the displacement vectors in a desired time window, we first determine the data variance for each component from the differences between daily displacements and a moving, locally weighted LOESS function (i.e. second-order polynomial regressions with a half-window time support). Then, all data points that exhibit differences exceeding two standard deviations are dismissed. Once the outliers have been

removed, a new regression is performed to estimate the final displacement vectors (e.g., Figure 1).

Figure 2

Following Villafuerte et al. (2025), we applied a seasonal noise reduction to all GPS data. This technique identifies and removes seasonal oscillations related to the Earth's elastic response to hydrological processes occurring on the surface, which may be particularly large in the vertical components (Heki, 2001). We assume that these oscillations can be modelled as a linear combination of two annual and two semi-annual trigonometric terms (Bevis and Brown, 2014). We therefore assume that the GPS time series during inter-SSE periods can be modelled as the sum of a secular linear function and the seasonal contributions. The method performs a multi-inter-SSE-window least-squares inversion to estimate the coefficients of each contribution and then subtracts the seasonal model from the displacement time series. Figures 2 and S1 illustrate this procedure at several stations, including the removal of outliers, where we can clearly appreciate how the technique allows identifying noise-hidden tectonic signals, particularly on the vertical component (Figure 2c).

2.2. Inversion Method

Inversions of the SSEs were performed using ELADIN (ELastostatic ADjoint INversion) (Tago et al., 2021), a well-established method for imaging slip at the plate interface from geodetic data with physically consistent constraints such as rake angle, admissible backslip, and spectral content considering three-dimensional fault geometries (Aguilar-Velázquez et al., 2025; Cruz-Atienza et al., 2025, 2021; Villafuerte et al., 2025). The plate interface has been discretized with 10 km x 10 km subfaults, assuming a geometry that incorporates the most recent seismotectonic information available for both states of Guerrero and Oaxaca (Cruz-Atienza et al., 2021). Since we deal with historic SSEs where station coverage has changed significantly over time, we tested different model regularizations to achieve optimal resolution as explained below. ELADIN handles the regularization by projecting the problem solutions into a spectrally constrained space given by the von Karman correlation function (Mai and Beroza, 2002). While we explored several correlation lengths of this function, the Hurst exponent was fixed at 0.75 according to previous work in the same area (Cruz-Atienza et al., 2025, 2021; Villafuerte et al., 2025). For all inversions, the Somigliana Green's functions were computed using the Okada model (Okada, 1992) assuming a half-space with crustal rigidity of 32×10^9 Pa.

3. Results

3.1. Slow slip events in the long term

To illustrate the outcome of the inversion procedure, Figure 3 presents the results obtained for the 2006 SSE in Guerrero, which has been the subject of substantial research (Cavalié et al., 2013; Radiguet et al., 2011; Tago et al., 2021). As transient SSE displacements begin and end at different times across the GPS network, the displacement time series were carefully discretized into sub-SSE windows (Figure 3 panels a and b), so that the total slip of the event is the sum of all inverted windows (Figure 3 panel c). The green dashed contour in panel c delineates the 70% resolution limit assuming an optimal correlation length of 40 km for

regularization purposes, determined from a Mobile Checkerboard (MOC) resolution test with 100 km unit size (Figure 3 panel d) (Tago et al., 2021). Please note that the majority of the inverted slip falls within this limit, indicating that the solution has a nominal error of less than 30% for slip patches larger than 100 km. As the MOC test did not include random noise, we would expect this resolution limit to be a lower bound with realistic values no upper than 40% (Tago et al., 2021).

Figure 3

Figures S2 and S3 show the inversion results for all analyzed SSEs together with their resolution analysis using MOC tests. Ten SSEs have been inverted in Guerrero since 2001 and five SSEs in Oaxaca since 2017, a complete catalogue in Guerrero since 2001. The solutions from 2021 in Guerrero were taken from Cruz-Atienza et al. (2025) while those between 2017 and 2020 in Oaxaca were taken from Villafuerte et al. (2025). Except for the 2001-2002 SSE, where only 6 GPS stations are available (Figure S3), all MOC tests were performed assuming unit slip patches of 100 km (and 150 km for the 2001-2002 event). In all SSE inversions, the final slip distributions are largely within the 70% resolution contour determined from the MOC tests, assuming an optimal correlation length for the von Karman regularization of 40 km, so we expect a nominal error of less than 30% within this limit, as mentioned earlier for the 2006 SSE.

Figure 4

Figure 4 shows the slip distribution of all SSEs within the 2 cm slip contour. In this figure, only the SSEs that initiated and developed spontaneously are considered, i.e. not triggered or affected by a large earthquake. Therefore, the 2014 and 2021 Guerrero SSEs (G-SSE5 and G-SSE10 in Table 1), when the Papanoa and Acapulco earthquakes occurred, respectively, are excluded to avoid the overlapping of the afterslip signatures (Cruz-Atienza et al., 2025; Radiguet et al., 2016). In Guerrero, where the instrumental coverage in recent years has allowed a much better illumination of the interface, including seafloor geodetic data (Cruz-Atienza et al., 2018a), two shallow and mostly offshore SSEs in 2021 and 2022 were found (G-SSE9 and G-SSE11; green shades in Figure 4) (Cruz-Atienza et al., 2025). The offshore SSEs south of the 2020 Huatulco earthquake in Oaxaca were determined by Villafuerte et al. (2025) (Figure 4).

Table 1

Except for the shallow events (green shades in Figure 4), all SSEs in both states correspond to long-term events and their slip distributions have been averaged to produce the blue contours of Figure 4 indicating the 15%, 40% and 80% slip iso-values. Three observations stand out from this figure: (1) a segmentation of the SSEs along the strike is clear with two maxima, one in Guerrero to the west and the other in Oaxaca to the east; (2) the maximum slip in Guerrero is significantly larger than that in Oaxaca, with both maxima between 30 and 40 km depth; and (3) the SSEs in Guerrero along the seismic gap reach shallow depths of ~13 km offshore, which correspond to seismogenic depths outside the gap. Figure 5 illustrates the along-trench extent and timing of all known SSEs in both states, together with the recent M7+ earthquakes in the region, whose locations are indicated in Figure 4. Events identified by a question mark in

Oaxaca denote instances where no inversion was possible, and thus the spatial extent is merely indicative. The timing of these events was estimated directly from the GPS record at station PINO, shown in Figures 1 and 4. Table 1 reports the limiting dates and magnitudes (if available) determined from the 1 cm slip contour for all SSEs in our catalog.

Figure 5

4. Discussion

The long-term SSEs in south-central Mexico demonstrate a clear segmentation along the strike between the Guerrero and Oaxaca regions. Only two of the fifteen events analyzed were found to span both regions. The maximum slip of all SSEs is statistically between 30 and 40 km depth (Figure 6). In contrast to the Oaxaca events with depths deeper than 20 km, Guerrero exhibits a different pattern where the up-dip slip limit extends to offshore regions, to approximately 20 km from the shoreline, reaching shallow depths of ~13 km in the Guerrero seismic gap (Figure 6). This condition, in conjunction with the recently discovered shallow SSEs, could account for the absence of major earthquakes in the seismic gap since 1911 (Cruz-Atienza et al., 2025). Such anomalous behavior could be associated with the presence of subducted bathymetry producing stable mechanical conditions (Plata-Martinez et al., 2024; Wang and Bilek, 2011), together with overpressured fluids at the plate contact as a consequence of the impermeable geology of the continental lower crust (Husker et al., 2018). SSEs in Guerrero are significantly larger than in Oaxaca. The discrepancy in magnitude appears to be attributable to the geometry of the plate interface. In Guerrero, the interface is subhorizontal and more extensive at depths prone to SSEs (i.e., between ~20 and ~45 km). In Oaxaca, though, the interface becomes gradually steeper, thereby reducing the extent of the SSE habitat.

The along-strike segmentation and extent of the SSEs' slip areas in south-central Mexico may depend on the morphology of both the subducting Cocos plate and the interface between the Cocos and North American plates. The seafloor spreading magnetic-anomalies and the bathymetric data between the East Pacific Rise and the Middle American Trench (MAT) reveal a very rich and complex tectonic history (e.g., Klitgord and Mammerickx, 1982). Several prominent features have been identified as fracture zones in the Cocos plate that extend from the spreading center to the MAT. As illustrated in Figure 6, the Orozco and probably the O'Gorman fracture zones reach the MAT in south-central Mexico (Klitgord and Mammerickx, 1982), where the SSEs develop in the states of Guerrero and Oaxaca. These fractures are characterized by deep troughs in the bathymetric relief, which certainly have mechanical implications in the plates contact once subducted. When compared to the average slip distribution of the SSEs (Figure 6), the onshore projection of both fracture zones appears to delineate the extensive SSE region of Guerrero. Specifically, the Orozco fracture zone delineates the northwestern boundary of the SSEs, while the O'Gorman fracture zone (while its trace is uncertain in the bathymetry and magnetic lineations, e.g., Klitgord and Mammerickx, 1982) may be implicated in the delineation of the Guerrero-Oaxaca SSEs segmentation near the state boundary.

Figure 6

Compared to some previous studies where different SSEs in Guerrero have been investigated, the moment magnitudes of the events determined in this study are significantly lower. For instance, for the 2001, 2006, and 2010 SSEs in Guerrero (G-SSE2, G-SSE3 and G-SSE4 in Table 1), we found their moment magnitude to be Mw = 7.2, whereas Radiguet et al. (2012) determined a range of 7.5 to 7.6 for the same events. As outlined in Section 2.1, this discrepancy can be attributed to the significantly different approaches to handling GPS data in the two studies. The inter-SSE trend removal from the data followed by these authors eliminates the North American plate common reference throughout the stations array and produces a significant overestimation of the SSEs displacement offsets, as compared to the actual crustal rebound considered in this study. This practice consequently leads to an overestimation of the interface slip and to inconsistency between the GPS displacement vectors that may lead to unreliable slip distributions. Evidence of this occurrence can be found in the Tokai subduction zone, Japan, where the simultaneous inversion of the relaxing and stressing slip at the interface demonstrates that an SSE occurred between 2002 and 2004 has a magnitude $M_w = 6.6$ (Ochi and Kato, 2013), instead of 7.0-7.1 reported by several previous authors who removed the inter-SSE linear trend from the GPS data (see references in Ochi and Kato, 2013). It is noteworthy that the discrepancy of 0.4 units of magnitude is consistent with the difference observed between our estimates and those reported by Radiguet et al. (2012). Although unlikely, such discrepancy in our case could also be partly attributable to the difference in the crustal model, which we assumed to be homogeneous, in contrast to the layered medium used by the referred authors.

The last six M7+ earthquakes around the states of Guerrero and Oaxaca were preceded and likely triggered by SSEs in most cases. These events include the Mw7.5 2012, Ometepec (Graham et al., 2014), the Mw7.3 2014, Papanoa (Radiguet et al., 2016), the Mw7.1 2017, Puebla-Morelos (Cruz-Atienza et al., 2021), the Mw7.2 2018, Pinotepa (Cruz-Atienza et al., 2021), the Mw7.4 2020, Huatulco (Villafuerte et al., 2025), and the Mw7.0 2021, Acapulco (Cruz-Atienza et al., 2025) earthquakes (Figures 4 and 5). This finding suggests that seismic hazard may increase during the occurrence of SSEs. However, a simple inspection of the Mexican historical record since the discovery in 1997 of the SSEs (Lowry et al., 2001) (Figure 5) reveals that this cluster of large earthquakes arises after a protracted 17-year quiescent period that commenced following the 1995 rupture of the Mw7.3 Copala earthquake (Courboulex et al., 1997), in proximity to the border of the two states (Figure 6). This shows that SSEs in that quiet time frame did not trigger a major earthquake, indicating that transient slow slip seems to be a necessary but insufficient process to initiate large ruptures. This particular temporal pattern, in which earthquake clusters lasting approximately 15 years are preceded by a similar period of quiescence, has been observed in Mexico since 1800 (Singh et al., 1981) and suggests the existence of periodic regional loading and discharge of the subduction zone (Nocquet et al., 2016). During the active periods, the interface seismogenic segments appear to attain a state of critical stability in a synchronous manner, thereby rendering them susceptible to rupture triggered by perturbations from SSEs, as evidenced by observations spanning the period from 2012 to 2021 in Guerrero and Oaxaca.

Cruz-Atienza et al. (2021) made a notable observation regarding the regional change in the magnitude and recurrence interval of SSEs following the Mw8.2 Tehuantepec earthquake of September 8, 2017 (Figure 5), the largest earthquake ever recorded in Mexico (Melgar et al., 2018; Suárez et al., 2019). The seismic waves from the event produced dynamic stress

perturbations at the interface of approximately 100 kPa for over 70 seconds in the vicinity of Acapulco, more than 600 km away from the earthquake. These transient perturbations triggered an SSE in Oaxaca and disrupted the mechanical properties of the plate interface on a regional scale over the subsequent two years (Cruz-Atienza et al., 2021). As illustrated in Figure 5, the consequences of this phenomenon can be seen in the aftermath of the Tehuantepec earthquake, where the average recurrence period of SSEs in Guerrero reduced to 0.4 years (in contrast to their characteristic 3.5 years since 1997) and the magnitude decreased from 7.2 to 6.9-7.0 (Table 1). These processes took place after the 17-year quiescent period in the subduction zone, during which energy accumulation in Guerrero and Oaxaca was sustained (Figure 1). The sequence of earthquakes that began in 2012 led to a transformation of the regional deformation regime. While the effective strain rate has remained negligible in the Guerrero seismic gap (station CAYA, Figure 1), in Oaxaca, the effective relaxation near Pinotepa Nacional in the same period is much higher (station PINO, Figure 1). This means that the occurrence of similar earthquakes in both states has different implications for energy release, which may be partly explained by the long-term effect of the SSEs in both regions, which are much larger in Guerrero, and by the postseismic relaxation of the earthquakes, which is much longer and pronounced in Oaxaca.

5. Conclusions

We have constructed a catalogue containing all known SSEs in south-central Mexico since 1997. The catalogue comprises a total of 11 events in Guerrero and 14 in Oaxaca. In the case of Oaxaca, the catalogue is presumably complete as of 2002. For this, we reported inversions of 15 SSEs made from a consistent treatment of GPS data and the same inversion technique (i.e. the ELADIN method; Tago et al., 2021). The GPS data have been curated to minimize seasonal noise caused by hydrometeorological loading (Villafuerte et al., 2025). This methodology is based on the characterization of noise during inter-SSE periods from annual and semi-annual harmonic functions, and is very effective for the recovery of tectonic signals, especially in the vertical component. Furthermore, the GPS displacements induced by the SSEs were estimated in the same North American reference frame in such a way that they correspond to the actual elastic rebound of the crust. This is in contrast to other studies in which such reference is removed, leading to an overestimation of the displacements.

We found a clear along-strike segmentation of the SSEs between the states of Guerrero and Oaxaca. This segmentation and the extent of slow events in Guerrero can be explained by structural control associated with the subduction of the Orozco and O'Gorman fracture zones in the Cocos plate. The onshore extensions of these fracture zones delimit the most active regions of SSEs in Guerrero to the northwest and southeast. Statistically, maximum slow slips are found between 30 and 40 km depth in both Guerrero and Oaxaca, with a much greater extent in Guerrero, determined by the subhorizontal geometry of the plate interface in that state that produces a more extensive SSE habitat. SSEs in Guerrero are thus significantly larger, with $M_w = 7.14 \pm 0.18$ and a duration of 10.3 ± 6.5 months, whereas in Oaxaca, $M_w = 6.84 \pm 0.16$ with a duration of 7.0 ± 4.3 months. In contrast to the rest of the region, where SSEs occur at depths below 20 km onshore, the SSEs in the Guerrero seismic gap reach shallow depths of ~13 km offshore, which corresponds to seismogenic depths outside the seismic gap. This phenomenon can be attributed to the presence of overpressured fluids at the plate interface, resulting from subducting bathymetry and an impermeable continental lower crust.

The last 28 years in south-central Mexico (i.e. since the discovery of SSEs in Mexico in 1997) are characterized by an initial seismic quiescence period (when large SSEs occurred), which ended with the Ometepec earthquake in 2012, and a subsequent seismically active period during which six M7+ earthquakes have occurred in the region. All earthquakes were preceded and likely triggered by an SSE, with the exception of the 2020 Huatulco earthquake in Oaxaca, where the preceding SSE had no clear bearing on the rupture. This suggests that SSEs seem to be a necessary but not sufficient process for the initiation of large earthquakes. The historical record in Mexico since 1800 shows that major earthquakes tend to occur in clusters lasting approximately 15 years (Singh et al., 1981) suggesting that, after comparable periods of quiescence, the subduction zone attains phases of critical stability, during which disturbances caused by SSEs may potentially trigger large seismic events. This also suggest that the current period of seismic activity could come to an end within the next few years.

Declaration of competing interest

The authors declare no conflicts of interest relevant to this study.

Acknowledgments

This research was possible thanks to UNAM PAPIIT grants IN111524, IA104525 and IN107524. This work was supported by JST SATREPS Japan Grant Number JPMJSA2310.

References

Aguilar-Velázquez, M.J., Miranda-García, P., Cruz-Atienza, V.M., Solano-Rojas, D., Tago, J., Domínguez, L.A., Villafuerte, C., Espíndola, V.H., Bello-Segura, D., Quintanar-Robles, L., Perton, M., 2025. Interplay of slow-slip faults beneath Mexico City induces intense seismicity over months. Tectonophysics 902, 230659. https://doi.org/10.1016/J.TECTO.2025.230659

Audet, P., Kim, Y.H., 2016. Teleseismic constraints on the geological environment of deep episodic slow earthquakes in subduction zone forearcs: a review. Tectonophysics 670, 1–15. https://doi.org/10.1016/j.tecto.2016.01.005

Bevis, M., Brown, A., 2014. Trajectory models and reference frames for crustal motion geodesy. J Geod 88, 283–311. https://doi.org/10.1007/S00190-013-0685-5/TABLES/2

Brudzinski, M., Cabral-Cano, E., Correa-Mora, F., Demets, C., Márquez-Azúa, B., 2007. Slow slip transients along the Oaxaca subduction segment from 1993 to 2007. Geophys. J. Int. 171, 523–538. https://doi.org/10.1111/j.1365-246x.2007.03542.x

Cabral-Cano, E., Pérez-Campos, X., Márquez-Azúa, B., Sergeeva, M.A., Salazar-Tlaczani, L., DeMets, C., Adams, D., Galetzka, J., Hodgkinson, K., Feaux, K., Serra, Y.L., Mattioli, G.S., Miller, M., 2018. TLALOCNet: a continuous GPS-Met Backbone in Mexico for seismotectonic and atmospheric research. Seismol. Res. Lett. 89, 373–381. https://doi.org/10.1785/0220170190

Cavalié, O., Pathier, E., Radiguet, M., Vergnolle, M., Cotte, N., Walpersdorf, A., Kostoglodov, V., Cotton, F., 2013. Slow slip event in the Mexican subduction zone: Evidence of shallower slip in the Guerrero seismic gap for the 2006 event revealed by the joint

420 inversion of InSAR and GPS data. Earth Planet Sci Lett 367, 52–60.
https://doi.org/10.1016/J.EPSL.2013.02.020
422 Correa-Mora, F., DeMets, C., Cabral-Cano, E., Diaz-Molina, O., Marquez-Azua, B., 2009.
Transient deformation in southern Mexico in 2006 and 2007: Evidence for distinct deep-
424 slip patches beneath Guerrero and Oaxaca. Geochemistry, Geophysics, Geosystems 10.
https://doi.org/10.1029/2008GC002211
426 Correa-Mora, F., Demets, C., Cabral-Cano, E., Marquez-Azua, B., Diaz-Molina, O., 2008.
Interplate coupling and transient slip along the subduction interface beneath Oaxaca,
428 Mexico. Geophys J Int 175, 269–290. https://doi.org/10.1111/J.1365-
246X.2008.03910.X/3/175-1-269-FIG017.JPEG
430 Cotte, N., Walpersdorf, A., Kostoglodov, V., Vergnolle, M., Santiago, J.A., Manighetti, I.,
Campillo, M., 2011. Anticipating the Next Large Silent Earthquake in Mexico. Eos,
432 Transactions American Geophysical Union 90, 181–182.
https://doi.org/10.1029/2009EO210002
434 Courboulex, F., Santoyo, M.A., Pacheco, J.F., Singh, S.K., 1997. The 14 September 1995 (M =
7.3) Copala, Mexico, earthquake: A source study using teleseismic, regional, and local
436 data. Bulletin of the Seismological Society of America 87, 999–1010.
https://doi.org/10.1785/BSSA0870040999
438 Cruz-Atienza, V.M., Ito, Y., Kostoglodov, V., Hjörleifsdóttir, V., Iglesias, A., Tago, J., Calò, M.,
Real, J., Husker, A., Ide, S., Nishimura, T., Shinohara, M., Mortera-Gutierrez, C., García, S.,
440 Kido, M., 2018a. A seismogeodetic amphibious network in the Guerrero Seismic Gap,
Mexico. Seismological Research Letters 89. https://doi.org/10.1785/0220170173
442 Cruz-Atienza, V.M., Tago, J., Domínguez, L.A., Kostoglodov, V., Ito, Y., Ovando-Shelley, E., et al.,
2025. Seafloor Geodesy Unveils Seismogenesis of Large Subduction Earthquakes in
444 México. Accepted in Science Advances 1–39.
Cruz-Atienza, V.M., Tago, J., Villafuerte, C., Wei, M., Garza-Girón, R., Dominguez, L.A.,
446 Kostoglodov, V., Nishimura, T., Franco, S.I., Real, J., Santoyo, M.A., Ito, Y., Kazachkina, E.,
2021. Short-term interaction between silent and devastating earthquakes in Mexico. Nat
448 Commun 12. https://doi.org/10.1038/s41467-021-22326-6
Cruz-Atienza, V.M., Villafuerte, C., Bhat, H.S., 2018b. Rapid tremor migration and pore-
450 pressure waves in subduction zones. Nat Commun 9. https://doi.org/10.1038/s41467-
018-05150-3
452 Fasola, S., Brudzinski, M.R., Ghouse, N., Solada, K., Sit, S., Cabral-Cano, E., Arciniega-Ceballos,
A., Kelly, N., Jensen, K., 2016. New perspective on the transition from flat to steeper
454 subduction in Oaxaca, Mexico, based on seismicity, nonvolcanic tremor, and slow slip. J
Geophys Res Solid Earth 121, 1835–1848. https://doi.org/10.1002/2015JB012709
456 Franco, S.I., Kostoglodov, V., Larson, K.M., Manea, V.C., Manea, M., Santiago, J.A., 2005.
Propagation of the 2001-2002 silent earthquake and interplate coupling in the Oaxaca
458 subduction zone, Mexico. Earth, Planets and Space 57, 973–985.
https://doi.org/10.1186/BF03351876/METRICS
460 Graham, S., DeMets, C., Cabral-Cano, E., Kostoglodov, V., Rousset, B., Walpersdorf, A., Cotte,
N., Lasserre, C., McCaffrey, R., Salazar-Tlaczani, L., 2016. Slow Slip History for the
462 MEXICO Subduction Zone: 2005 Through 2011. Pure Appl. Geophys. 173, 3445–3465.
https://doi.org/10.1007/s00024-015-1211-x
464 Graham, S.E., DeMets, C., Cabral-Cano, E., Kostoglodov, V., Walpersdorf, A., Cotte, N.,
Brudzinski, M., McCaffrey, R., Salazar-Tlaczani, L., 2014. GPS constraints on the 2011-

2012 Oaxaca slow slip event that preceded the 2012 March 20 Ometepec earthquake, southern Mexico. Geophys J Int 197, 1593–1607. https://doi.org/10.1093/GJI/GGU019

Heki, K., 2001. Seasonal Modulation of Interseismic Strain Buildup in Northeastern Japan Driven by Snow Loads. Science (1979) 293, 89–92. https://doi.org/10.1126/SCIENCE.1061056

Husker, A., Ferrari, L., Arango-Galván, C., Corbo-Camargo, F., Arzate-Flores, J.A., 2018. A geologic recipe for transient slip within the seismogenic zone: Insight from the Guerrero seismic gap, Mexico. Geology 46, 35–38. https://doi.org/10.1130/G39202.1

Iglesias, A., Singh, S.K., Lowry, A.R., Santoyo, M., Kostoglodov, V., Larson, K.M., Franco-Sánchez, S.I., 2004. The silent earthquake of 2002 in the Guerrero seismic gap, Mexico (Mw=7.6): Inversion of slip on the plate interface and some implications. Geofísica Internacional 43, 309–317. https://doi.org/10.22201/IGEOF.00167169P.2004.43.3.953

Klitgord, K.D., Mammerickx, J., 1982. Northern East Pacific Rise: Magnetic anomaly and bathymetric framework. J Geophys Res Solid Earth 87, 6725–6750. https://doi.org/10.1029/JB087IB08P06725

Kostoglodov, V., Husker, A., Shapiro, N.M., Payero, J.S., Campillo, M., Cotte, N., Clayton, R., 2010. The 2006 slow slip event and nonvolcanic tremor in the Mexican subduction zone. Geophys Res Lett 37. https://doi.org/10.1029/2010GL045424

Kostoglodov, V., Singh, S.K., Santiago, J.A., Franco, S.I., Larson, K.M., Lowry, A.R., Bilham, R., 2003. A large silent earthquake in the Guerrero seismic gap, Mexico. Geophys Res Lett 30. https://doi.org/10.1029/2003GL017219

Lagler, K., Schindelegger, M., Böhm, J., Krásná, H., Nilsson, T., 2013. GPT2: Empirical slant delay model for radio space geodetic techniques. Geophys. Res. Lett. 40, 1069–1073. https://doi.org/10.1002/grl.50288

Larson, K.M., Kostoglodov, V., Miyazaki, S., Santiago, J.A.S., 2007. The 2006 aseismic slow slip event in Guerrero, Mexico: New results from GPS. Geophys Res Lett 34. https://doi.org/10.1029/2007GL029912

Legrand, D., Iglesias, A., Singh, S.K., Cruz-Atienza, V., Yoon, C., Dominguez, L.A., Valenzuela, R.W., Suárez, G., Castro-Artola, O., 2021. The influence of fluids in the unusually high-rate seismicity in the Ometepec segment of the Mexican subduction zone. Geophys J Int 226. https://doi.org/10.1093/gji/ggab106

Lowry, A.R., Larson, K.M., Kostoglodov, V., Bilham, R., 2001. Transient fault slip in Guerrero, southern Mexico. Geophys Res Lett 28, 3753–3756. https://doi.org/10.1029/2001GL013238

Mai, P.M., Beroza, G.C., 2002. A spatial random field model to characterize complexity in earthquake slip. J Geophys Res Solid Earth 107, ESE 10-1. https://doi.org/10.1029/2001JB000588

Manea, V.C., Manea, M., 2011. Flat-slab thermal structure and evolution beneath central Mexico. Pure Appl Geophys 168, 1475–1487. https://doi.org/10.1007/S00024-010-0207-9/FIGURES/6

Nocquet, J.M., Jarrin, P., Vallée, M., Mothes, P.A., Grandin, R., Rolandone, F., Delouis, B., Yepes, H., Font, Y., Fuentes, D., Régnier, M., Laurendeau, A., Cisneros, D., Hernandez, S., Sladen, A., Singaucho, J.C., Mora, H., Gomez, J., Montes, L., Charvis, P., 2016. Supercycle at the Ecuadorian subduction zone revealed after the 2016 Pedernales earthquake. Nature Geoscience 2017 10:2 10, 145–149. https://doi.org/10.1038/ngeo2864

Ochi, T., Kato, T., 2013. Depth extent of the long-term slow slip event in the Tokai district, central Japan: A new insight. J Geophys Res Solid Earth 118, 4847–4860. https://doi.org/10.1002/JGRB.50355

Okada, Y., 1992. Internal deformation due to shear and tensile faults in a half-space. Bulletin of the Seismological Society of America 82, 1018–1040. https://doi.org/10.1785/BSSA0820021018

Pardo, M., Suarez, G., 1995. Shape of the subducted Rivera and Cocos plates in southern Mexico: Seismic and tectonic implications. J Geophys Res Solid Earth 100, 12357–12373. https://doi.org/10.1029/95JB00919

Pérez-Campos, X., Kim, Y.H., Husker, A., Davis, P.M., Clayton, R.W., Iglesias, A., Pacheco, J.F., Singh, S.K., Manea, V.C., Gurnis, M., 2008. Horizontal subduction and truncation of the Cocos Plate beneath central Mexico. Geophys Res Lett 35. https://doi.org/10.1029/2008GL035127

Plata-Martinez, R., Iinuma, T., Tomita, F., Nakamura, Y., Nishimura, T., Hori, T., 2024. Revisiting Slip Deficit Rates and Its Insights Into Large and Slow Earthquakes at the Nankai Subduction Zone. J Geophys Res Solid Earth 129, e2023JB027942. https://doi.org/10.1029/2023JB027942

Radiguet, M., Cotton, F., Vergnolle, M., Campillo, M., Valette, B., Kostoglodov, V., Cotte, N., 2011. Spatial and temporal evolution of a long term slow slip event: The 2006 Guerrero Slow Slip Event. Geophys J Int 184, 816–828. https://doi.org/10.1111/J.1365-246X.2010.04866.X

Radiguet, M., Cotton, F., Vergnolle, M., Campillo, M., Walpersdorf, A., Cotte, N., Kostoglodov, V., 2012. Slow slip events and strain accumulation in the Guerrero gap, Mexico. J Geophys Res Solid Earth 117. https://doi.org/10.1029/2011JB008801

Radiguet, M., Perfettini, H., Cotte, N., Gualandi, A., Valette, B., Kostoglodov, V., Lhomme, T., Walpersdorf, A., Cabral Cano, E., Campillo, M., 2016. Triggering of the 2014 Mw7.3 Papanoa earthquake by a slow slip event in Guerrero, Mexico. Nat. Geosci. 9, 829–833. https://doi.org/10.1038/ngeo2817

Singh, S.K., Astiz, L., Havskov, J., 1981. Seismic gaps and recurrence periods of large earthquakes along the Mexican subduction zone: A reexamination. Bulletin of the Seismological Society of America 71, 827–843. https://doi.org/10.1785/BSSA0710030827

Tago, J., Cruz-Atienza, V.M., Villafuerte, C., Nishimura, T., Kostoglodov, V., Real, J., Ito, Y., 2021. Adjoint slip inversion under a constrained optimization framework: Revisiting the 2006 Guerrero slow slip event. Geophys J Int 226. https://doi.org/10.1093/gji/ggab165

Vergnolle, M., Walpersdorf, A., Kostoglodov, V., Tregoning, P., Santiago, J.A., Cotte, N., Franco, S.I., 2010. Slow slip events in Mexico revised from the processing of 11 year GPS observations. J Geophys Res Solid Earth 115, 8403. https://doi.org/10.1029/2009JB006852

Villafuerte, C., Cruz-Atienza, V.M., Tago, J., Solano-Rojas, D., Garza-Girón, R., Girón, G., Franco, S.I., Dominguez, L.A., Kostoglodov, V., 2025. Slow slip events and megathrust coupling changes contribute to the earthquake potential in Oaxaca, Mexico. Geophys J Int 241, 17–34. https://doi.org/10.1093/GJI/GGAF022

Walpersdorf, A., Cotte, N., Kostoglodov, V., Vergnolle, M., Radiguet, M., Santiago, J.A., Campillo, M., 2011. Two successive slow slip events evidenced in 2009–2010 by a dense GPS network in Guerrero, Mexico. Geophys Res Lett 38. https://doi.org/10.1029/2011GL048124

558 Wang, K., Bilek, S.L., 2011. Do subducting seamounts generate or stop large earthquakes? Geology 39, 819–822. https://doi.org/10.1130/G31856.1
560 Zumberge, J.F., Heflin, M.B., Jefferson, D.C., Watkins, M.M., Webb, F.H., 1997. Precise point positioning for the efficient and robust analysis of GPS data from large networks. J
562 Geophys Res Solid Earth 102, 5005–5017. https://doi.org/10.1029/96JB03860

564 **Figures and Tables**

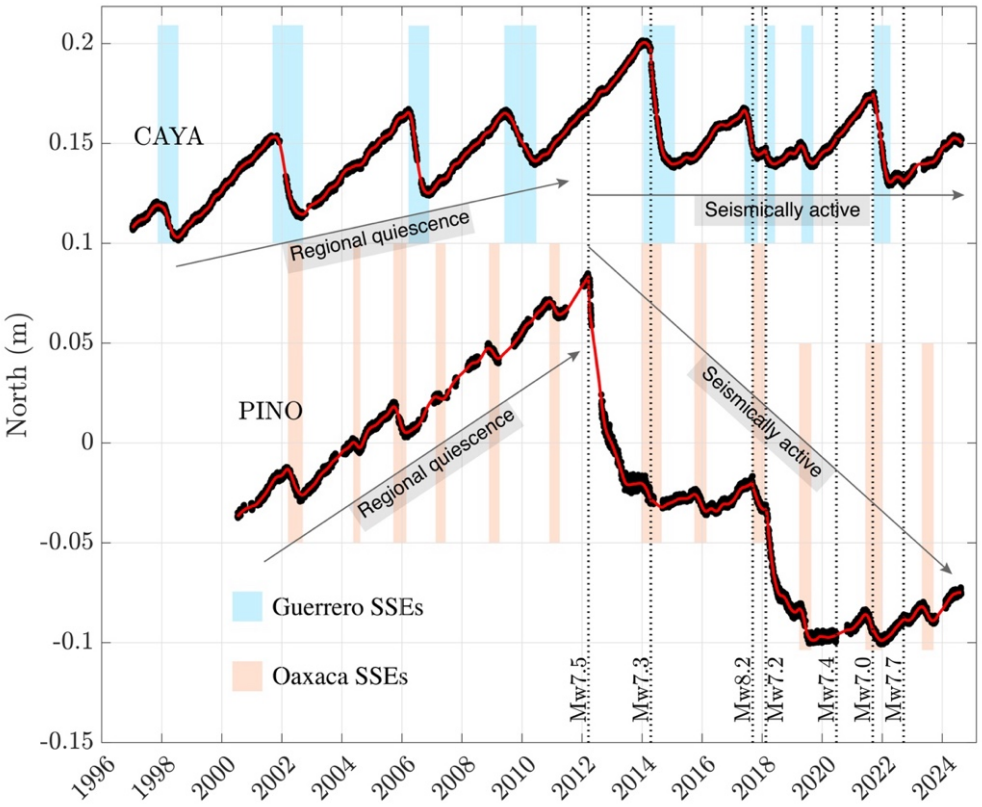

566 **Figure 1** Long-term GPS record at two permanent stations in the states of Guerreo and Oaxaca
568 (see Figure 4 for stations location). Arrows indicate the effective strain rate during phases of regional seismic quiescence (left) and seismic activity (right). Dashed lines indicate the dates
570 of all M7+ earthquakes in the region. Light blue and orange rectangles indicate the periods of SSEs in Guerrero and Oaxaca, respectively.

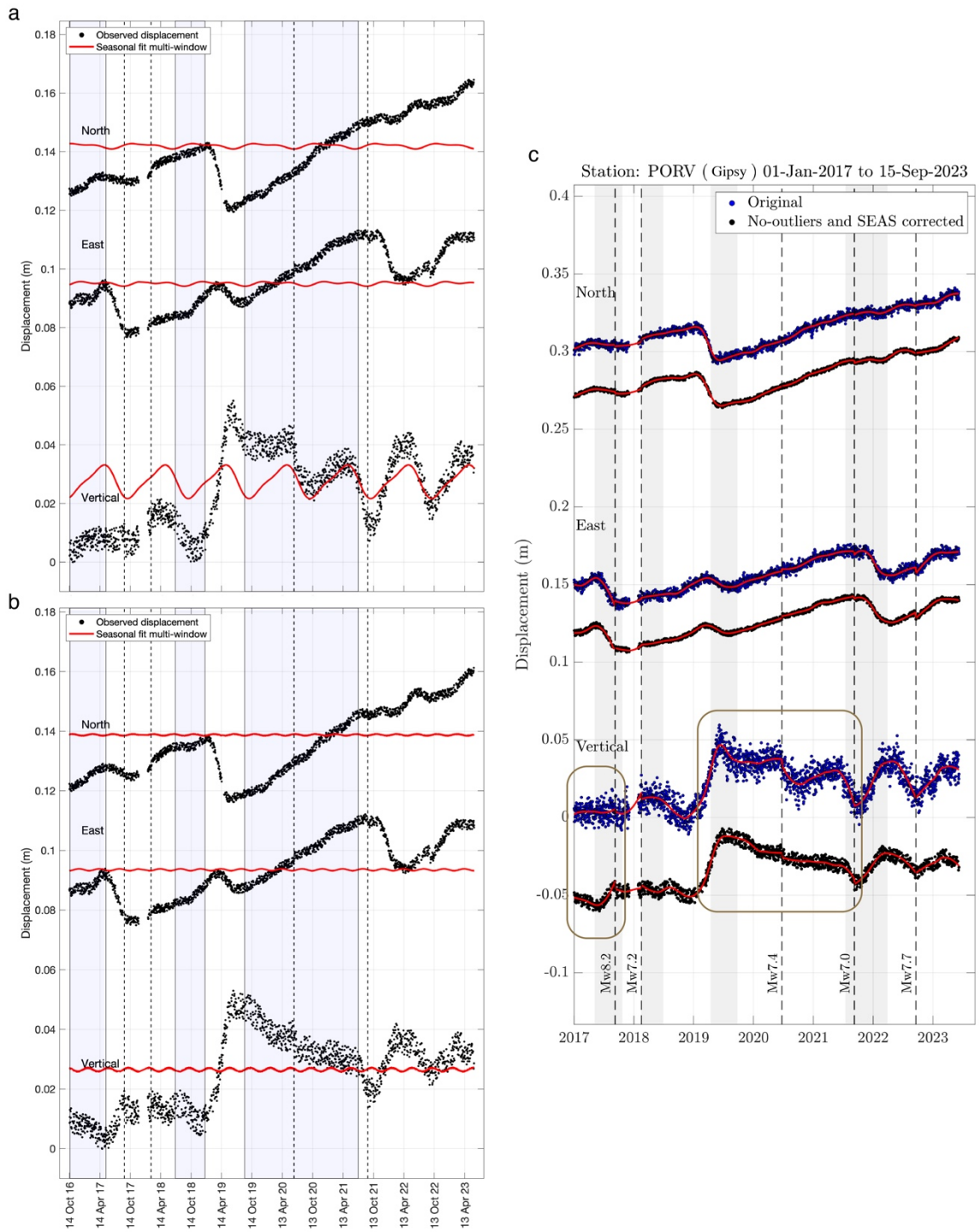

572

574 **Figure 2** Procedure for hydrometeorological (seasonal) noise reduction in GPS data (black and blue dots) at station PORV (Figure 4). (a and b) Best fitting annual and semi-annual harmonic
576 functions during inter-SSE periods (blue shades). (c) Comparison of raw data (blue dots) and seasonal noise corrected data with outliers removal (black dots) in their three components.
578 Other examples of this correction are shown in Figure S1.

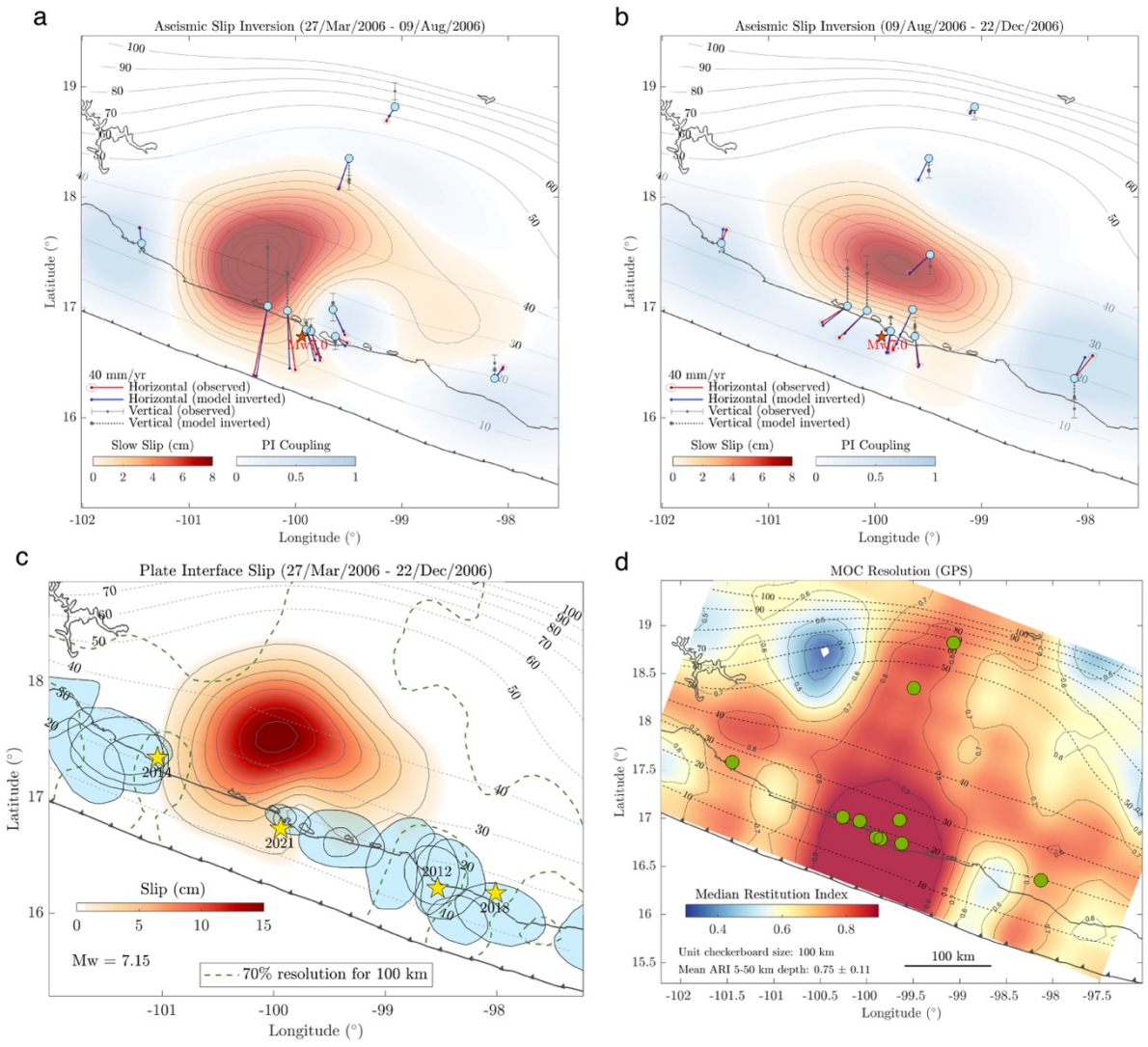

580

582 **Figure 3** Inversion of the 2006 SSE in Guerrero and resolution analysis. (a and b) Inverted
individual windows along with the misfit between the data (red arrows) and the model's
584 theoretical predictions (blue arrows). (c) Total slip associated with the 2006 SSE resulting from
the sum of the two inverted windows (panels a and b). (d) Median restitution index resulting
586 from a Mobile Checkerboard resolution test for a unit size of 100 km. Note that the 0.7 contour
is indicated in panel c (green dashed curve) and correspond to the boundary where nominal
588 error in less than 30%.

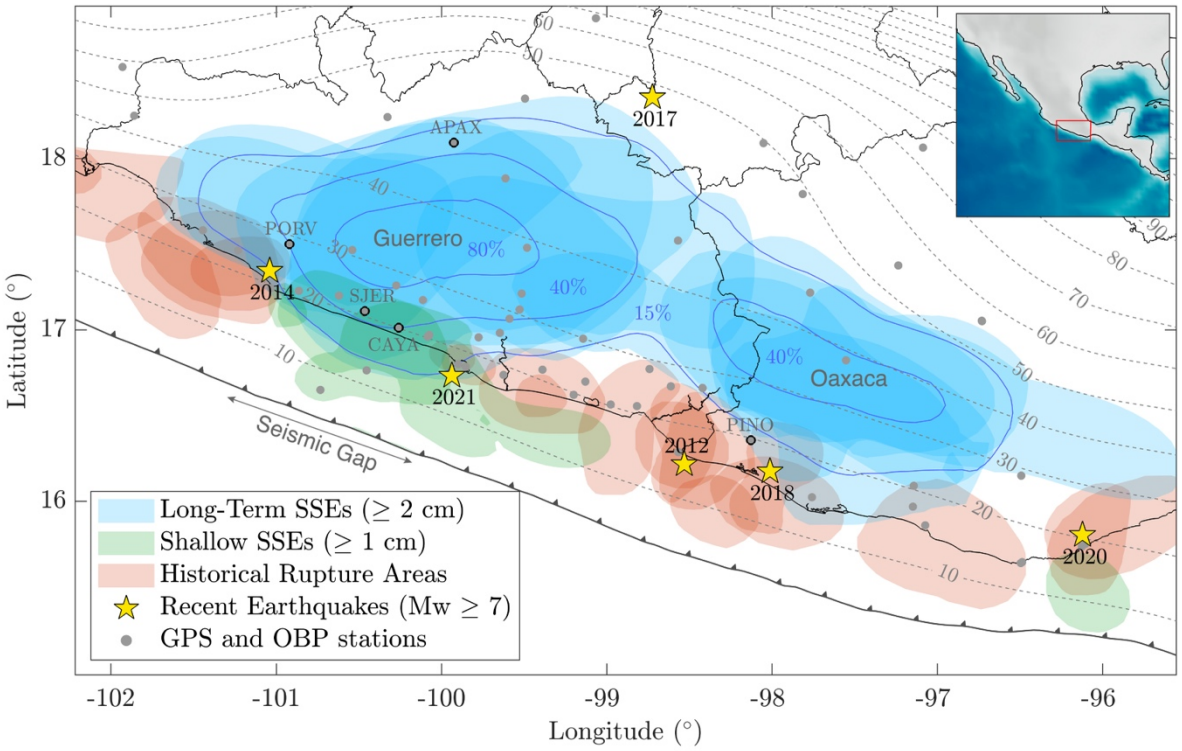

Figure 4 Slip distributions of all inverted SSEs (blue shades) between 2001 and 2023 along with the rupture areas of past earthquakes (red shades). The 2014 and 2021 SSEs in Guerrero were excluded to avoid the postseismic signatures of large nearby ruptures. Shallow SSEs in Guerrero follow Cruz-Atienza V.M. et al. (2025) while those in Oaxaca follow Villafuerte et al. (2025). The blue contours indicating percentages correspond to the proportion of cumulative slow slip. OBP means Ocean Bottom Pressure gauges. The extension of the Guerrero seismic gap is shown by a straight line offshore, between the epicenters of 2014 and 2021 earthquakes.

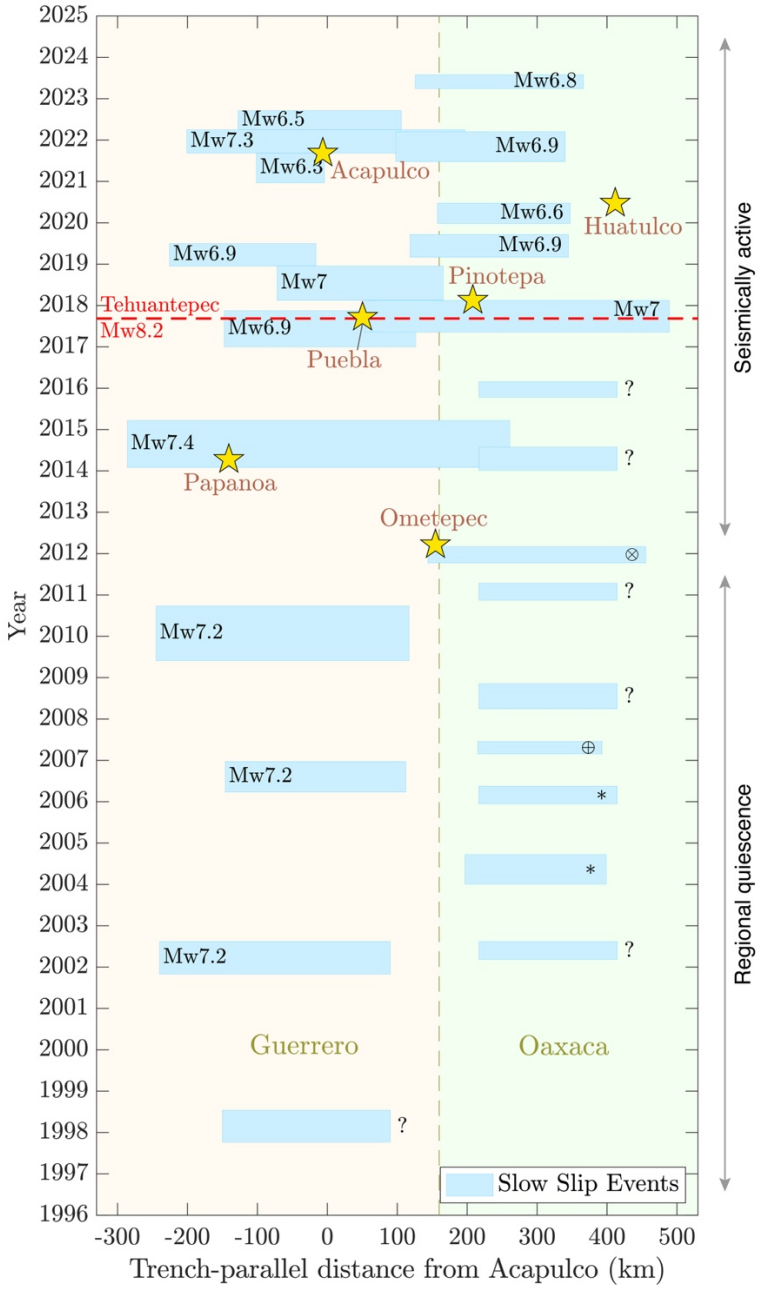

600

602 **Figure 5** Temporal distribution along the trench-parallel direction from Acapulco of all known SSEs and M7+ earthquakes in Guerrero and Oaxaca since 1996. Events with specified
604 magnitudes were inverted (see Table 1). The duration of SSEs with a question mark was determined from GPS records in Oaxaca, while their extent is only indicative. SSEs indicated
606 with ∗ are from Correa-Mora et al. (2008); with ⊗ from Correa-Mora et al. (2009), and with ⊕ from Graham et al. (2014).

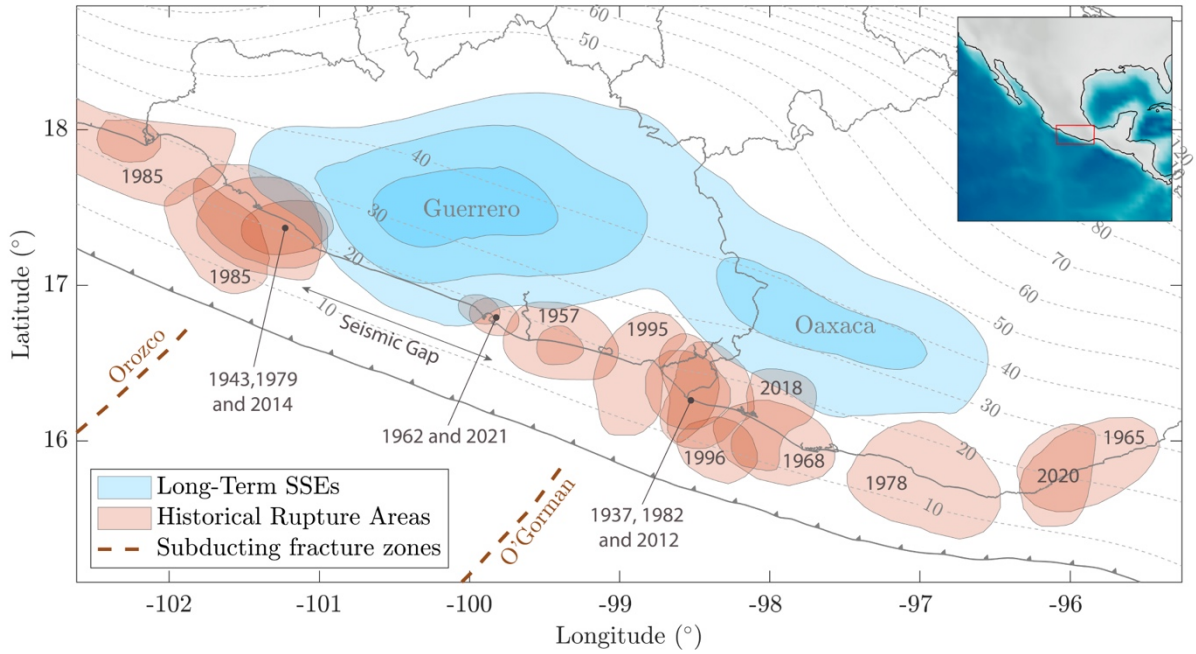

Figure 6 Average slip distribution of all inverted SSEs (shown in blue). The historic rupture areas and their years of occurrence are shown in red.

Guerrero SSEs				Oaxaca SSEs		
Label	Dates	Mw		Label	Dates	Mw
G-SSE1	Oct/1997 - Jul/1998	?		O-SSE1	Mar/2002 - Aug/2002	?
G-SSE2	Nov/2001 - Aug/2002	7.20		O-SSE2*	Jan/2004 - Sep/2004	~7.0
G-SSE3	Mar/2006 - Dec/2006	7.15		O-SSE3*	Dec/2005 - May/2006	~7.0
G-SSE4	Jun/2009 - Sep/2010	7.17		O-SSE4*	Feb/2007 - Jun/2007	~7.0
G-SSE5	Feb/2014 - Mar/2015	7.44		O-SSE5	Nov/2008 - Apr/2008	?
G-SSE6	Jan/2017 - Nov/2017	6.93		O-SSE6	Nov/2010 - Apr/2011	?
G-SSE7	Feb/2018 - Dec/2018	7.03		O-SSE7	Oct/2011 - Mar/2012	?
G-SSE8	Dec/2018 - Jul/2019	6.93		O-SSE8	Jan/2014 - Jul/2014	?
G-SSE9	Dec/2020 - Sep/2021	6.28		O-SSE9	Oct/2015 - Feb/2016	?
G-SSE10	Sep/2021 - Apr/2022	7.29		O-SSE10	May/2017 - Feb/2018	7.03
G-SSE11	Apr/2022 - Sep/2022	6.52		O-SSE11	Mar/2019 - Sep/2019	6.89
				O-SSE12	Dec/2019 - Jun/2020	6.62
				O-SSE13	Jun/2021 - Mar/2022	6.89
				O-SSE14	Apr/2023 - Aug/2023	6.75

Table 1 SSEs catalog in Guerrero and Oaxaca. Events with question mark were not inverted and their timings were determined from GPS records. G-SSE5 and GSSE10 include the afterslip signatures of the 2014 Papanoa and 2021 Acapulco earthquakes, while G-SSE9 and G-SSE11 are shallow events determined by Cruz-Atienza et al. (2025). The Oaxaca SSEs indicated with and asterisk (*) follow Graham et al. (2009).